Steel and Composite Structures, *Vol. 19*, *No. 6* (*2015*) *1467-1481*
DOI: http://dx.doi.org/10.12989/scs.2015.19.6.1467

Development of new predictive analysis in the orthogonal metal cutting process by utilization of Oxley's machining theory

Abdelkader Karas *[1,3], Mohamed Bouzit [2], Mustapha Belarbi [3] and Redha Mazouzi [1]

[1] *Khemis Miliana University*, *FIMA Laboratory*, *44225*, *Algeria*
[2] *Laboratory of Applied Mechanics*, *Faculty of Mechanical Engineering USTO-MB*, *Oran*, *Algeria*
[3] *University of Tiaret*, *Faculty of Sciences Appliquées*, *Algeria*

(*Received January 12*, *2015*, *Revised June 22*, *2015*, *Accepted June 23*, *2015*)

Abstract. This paper presents a contribution to improving an analytical thermo-mechanical modeling of Oxley's machining theory of orthogonal metals cutting, which objective is the prediction of the cutting forces, the average stresses, temperatures and the geometric quantities in primary and secondary shear zones. These parameters will then be injected into the developed model of Karas *et al*. (2013) to predict temperature distributions at the tool-chip-workpiece interface. The amendment to Oxley's modified model is the reduction of the estimation of time-related variables cutting process such as cutting forces, temperatures in primary and secondary shear zones and geometric variables by the introduction the constitutive equation of Johnson-Cook model. The model-modified validation is performed by comparing some experimental results with the predictions for machining of 0.38% carbon steel.

Keywords: orthogonal metals cutting; Oxley's theory; analytical modeling; Johnson-Cook model; temperature distributions

1. Introduction

Cutting metals is a complex phenomenon to model because of the strong nonlinearities induced as well as mechanical and thermal effects that are extremely linked. From a mechanical point of view, this complexity is related to large deformations and strain rates and nature of contacts with tool-chip and tool-workpiece interfaces. In addition to these mechanical effects, local heat generation and strong temperature gradient added due to the conversion of plastic deformation and friction energy.

Since the work of Merchant (1945), several modeling of the formation chips in orthogonal cutting were developed in order to understand the physical phenomena involved and to determine the mechanical, thermal and geometrical quantities associated with the deformation zones. The thermomechanical model most commonly encountered is that of Oxley (1989); it allows, from the knowledge of cutting conditions and the rheological law milled material, the prediction of cutting forces, mean stresses, strains, strain rates, average temperatures and geometric quantities such as

∗Corresponding author, Ph.D., E-mail: karasaek@yahoo.fr
[a] Ph.D., E-mail: karasaek@yahoo.fr

http://www.techno-press.org/?journal=scs&subpage=8 ISSN: 1229-9367 (Print), 1598-6233 (Online)

shear angle, chip thickness and its tool-chip interface length, and the undeformed chip thickness.

Despite the average values of the temperature provided by Oxley's model, determination of its maximum value and its distribution is of particular interest to ensure the longevity of tools and ensure the quality of manufactured product; but its knowledge is very difficult analytically and experimentally. For this purpose, different analytical models and measuring methods have been developed to characterize the heat transfer in the deformation zones. Pioneering studies were performed by Hahn (1951), Trigger and Chao (1951), Loewen and Shaw (1954), Chao and Trigger (1995), Komanduri and Hou (2001, 2001a, b), Karpat and Özel (2006), Karas *et al*. (2013), Klocke *et al*. (2014), Gierlings and Brockmann (2013, 2014) and Bogdan and Milan (2014).

Adibi-Sedeh *et al*. (2003) extended Oxley's machining theory for prediction of cutting forces and temperatures with few different assumptions for various material models namely Johnson–Cook material model, history dependent power law model and mechanical threshold stress model. Lalwani *et al*. (2009) and Liangshan *et al*. (2014) simply inherited original algorithm in their extended models. Some Improvements to the Oxley's model were subsequently made while changing, for example, the rheological law of the machined material to use it in the simulation of High Speed Cutting. Due to this, the rheological law, which is currently the most used, is that of Johnson-Cook (1983) that makes it easy to predict and more realistically the rheological behavior of a variety of materials in machining. Determining the parameters A, B, C, n and m is performed using the dynamic tests generally based on the technique of Split Hopkinson Pressure Bar (SHPB).

As from the use of the test results on the orthogonal section whose contents included cutting forces F_c and thrust force F_t values and the chip thickness; it is proposed in this work to determine the constants in the constitutive equation of Johnson-Cook model by applying the analysis of Oxley slip lines of field.

In this study, the constants of Johnson-Cook model are determined by using a nonlinear regression solution based on the Gauss-Newton algorithm with Levenberg-Marquardt modifications Bates and Wattes (1988) for better global convergence.

What is also interesting and original in this work is that it is use of the Oxley's model while integrating rheological law of Johnson-Cook model to predict the cutting forces, the average stresses, temperatures and the geometric quantities; the amendment also made to the Oxley model concerns the reduction of time estimation variables related to cutting process such as cutting forces, temperatures at the primary and secondary shear zones and geometry of the chip; subsequently these estimates will be injected into the developed model of Karas *et al*. (2013) based on the principle of a moving heat source for developing the temperature distributions in the tool-chip-workpiece interface.

2. Description of Oxley's machining theory

The thermomechanical model of Oxley (1989) is the combination of two parts: the first part is mechanically using the slip-set method; the second part is thermal after work to Boothroyd (1963). Following earlier developments, Oxley considers that the primary shear occurs in the zone of a certain thickness and not abruptly, and the contact conditions at the tool-chip interface corresponds to a sticky contact; the latter case leads to the formation of a secondary shear zone. The Fig. 1 shows the primary and secondary shear zones.

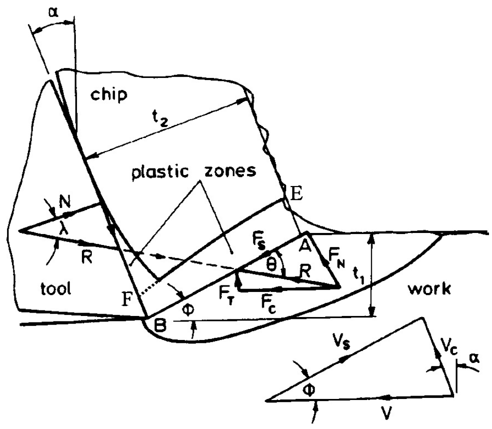

Fig. 1 Chip formation model (Oxley 1989)

We must determine the flow stress in each of these zones, which amounts to estimating the strain, strain rate and temperature, and then write two equilibrium relations (forces and moments) and energy relationship for the minimization of the power loss in order to obtain the unknowns of the problem; namely, the primary shear angle (ϕ), strain rate constant proposed by Oxley (C_o) and ratio of tool-chip interface plastic zone thickness to chip thickness (δ) Gilormini (1982).

The basic of the theory is to analyze the tress the stress distribution along shear plane *AB* and at the tool-chip interface in terms of the shear angle ϕ and workpiece material properties. Then, to select ϕ so that the resultant forces transmitted by shear plane *AB* and the tool-chip interface are in equilibrium once ϕ is known then the chip thickness and force components can be determined from the geometric relations

$$t_2 = t_1 \cos(\phi - \alpha) / \sin\phi \tag{1}$$

$$F_c = R\cos(\lambda - \alpha) \tag{2}$$

$$F_t = R\sin(\lambda - \alpha) \tag{3}$$

$$F = R\sin\lambda \tag{4}$$

$$N = R\cos\lambda \tag{5}$$

$$R = \frac{F_s}{\cos\theta} = \frac{k_{AB} t_1 w}{\sin\phi\cos\theta} \tag{6}$$

By applying the appropriate stress equilibrium equation along shear plane *AB*, it can be shown that the angle θ between resultant force *R* and *AB* is as follows

$$\tan(\theta) = 1 + 2 \cdot (0.25\pi - \phi) - C_0 \cdot n \tag{7}$$

The constant C_0 obtained from the empirical strain-rate relation

$$\dot{\gamma}_{AB} = C_0 V_s / l \tag{8}$$

The angle θ is can also be related to other angles as shown in the geometry of Fig. 1.

$$\theta = \phi + \lambda - \alpha \tag{9}$$

Therefore, the equivalent strain and strain-rate using von Mises criterion are

$$\varepsilon_{AB} = \gamma_{AB} / \sqrt{3} \tag{10}$$

$$\dot{\varepsilon}_{AB} = \dot{\gamma}_{AB} / \sqrt{3} \tag{11}$$

The temperature at shear plane AB to determine flow stress at shear plane together with the strain-rate and strain is found from the equation

$$T_{AB} = T_w + \eta \frac{(1-\beta) F_s \cos\alpha}{\rho C_p t_1 w \cos(\phi - \alpha)} \tag{12}$$

Where β is a portion of heat conducted to the workpiece from the shear zone and is given by the equations

$$\begin{aligned} &\beta = 0.5 - 0.35 \log\left(R_T \tan\phi\right) && 0.04 \le R_T \tan\phi \le 10.0 \\ &\beta = 0.5 - 0.15 \log\left(R_T \tan\phi\right) && R_T \tan\phi \succ 10.0 \end{aligned} \tag{13}$$

With R_T a non-dimensional thermal number given by

$$R_T = \rho C_p V_C t_1 / K \tag{14}$$

The limits, $0 \le \beta \le 1$, are also imposed. The strain at AB is given by

$$\gamma_{AB} = \frac{1}{2} \frac{\cos\alpha}{\sin\phi \cos(\phi - \alpha)} \tag{15}$$

The average temperature at the tool-chip interface from which the average shear flow stress at the interface is determined as

$$T_{int} = T_w + \frac{(1-\beta)}{\rho C_p t_1 w} \frac{F_s \cos\alpha}{\cos\left(\phi - \alpha\right)} + \psi \, \Delta T_M \tag{16}$$

Tint being an average value. If the thickness of the plastic zone is taken as δt_2, where δ is the ratio of this thickness to the chip thickness t_2, then

$$\log\left(\frac{\Delta T_M}{\Delta T_C}\right) = 0.06 - 0.195\,\delta \sqrt{\frac{R_T t_2}{h}} + 0.5 \log\left(\frac{R_T t_2}{h}\right) \tag{17}$$

Where ΔT_C is the average temperature rise in the chip is given by

$$\Delta T_C = \frac{F\,sin\,\phi}{\rho\,C_p\,t_1\,w\,cos(\phi-\alpha)} \tag{18}$$

The tool-chip contact length h is given by

$$h = \frac{t_1\,sin\,\theta}{cos\,\lambda\,sin\phi}\left[1+\frac{C_0\,n}{3\left[1+2\left(\frac{1}{4}\pi-\phi\right)-C_0\,n\right]}\right] \tag{19}$$

The average shear strain rate and shear strain are considered constant and can be estimated from Eqs. (20)-(21) in the secondary zone

$$\dot{\gamma}_{int} = V/\delta t_2 \tag{20}$$

$$\gamma_{int} = h/\delta t_2 \tag{21}$$

The equivalent maximum strain and strain-rate at tool–chip interface using Von Mises Criterion are

$$\varepsilon_{int} = \gamma_{int}/\sqrt{3} \tag{22}$$

$$\dot{\varepsilon}_{int} = \dot{\gamma}_{int}/\sqrt{3} \tag{23}$$

After that point a range of shear angle ϕ is tried out until the resolved shear stress at the tool-chip interface that is expressed at Eq. (24) and the shear flow stress, k_{chip}, with the calculated strain rate $\dot{\gamma}_{\text{int}}$ and temperature T_{int} are in equilibrium (i.e., $\tau_{\text{int}} = k_{chip}$).

$$\tau_{int} = F/h\,w \tag{24}$$

Order to determine constant C_0, a stress boundary condition at the cutting edge B is considered and the average normal stress at the interface is given by

$$\sigma_N = N/h\,w \tag{25}$$

By using another stress boundary condition at B by working from A along AB, this stress can be expressed as

$$\sigma'_N/k_{AB} = 1+0.5\pi-2\alpha-2C_0\,n \tag{26}$$

C_0 can now be determined from the condition that σ_N and σ'_N must be equal. The constant δ that gives a combination of strain rate and temperature that minimizes the shear flow stress k_{chip} is found by satisfying both minimum frictional and deformation work conditions

In support of their developments, Oxley and Hastings (1975) used an empirical representation of the yield stress or the behavior law of the machined material given by

$$\sigma = \sigma_1(T_{mod})\cdot\varepsilon^{n(T_{mod})} \tag{27}$$

Note that uniaxial flow stress at $\varepsilon = 1$, (σ_1) and strain-hardening index (n) have nonlinear evolution according to the velocity-modified temperature (T_{mod}). Hastings *et al*. (1980) suggested the concept of the latter; the expression of velocity-modified temperature is given by

$$T_{mod} = T \cdot \left(1 - \nu \cdot log\left(\frac{\dot{\varepsilon}}{\dot{\varepsilon}_0}\right)\right) \tag{28}$$

ν and $\dot{\varepsilon}_0$ are constant for a given material.

The changes in the uniaxial flow stress (σ_1) and strain hardening index (n) depending on the velocity-modified temperature from compression tests on carbon steel (0.16 to 0.55% C) led by Oyane and co-authors (Hastings *et al*. (1980)), for a strain of 1, a strain rate of 450 s^{-1} and a temperature of 1100°C. Therefore, the concept of the velocity-modified temperature allowed an extrapolation of results for the compression tests of conditions for machining.

Oxley and co-workers developed a computer program to carry out the above analysis. It is found that the analysis yields results in good agreement with experiments. Typical values of these parameters used by Oxley and co-workers range from 0.5 to 1.0 for carbon steel.

In recent years, an extensive amount of characterization of material properties at high strain rate and temperature has been carried out for use in simulation of high velocity impacts. The Johnson-Cook model we widely used constitutive model for which the coefficients are available for a variety of materials.

3. Description of the material model used

During machining, the machined material undergoes deformations to the order of 200% and strain rates up to 10^5 s^{-1}, while Hopkinson Pressure Bar (SHPB) testing achieve deformations of the order of 100% and 10^3 s^{-1} strain rate; thus, it is difficult to arrive at a very satisfactory result because many physical phenomena generated in the deformation zones are coupled (shear and friction in the secondary shear zone, for example) and it is difficult to access all size (strain, strain rates, temperature,...) during machining. Some authors propose to use the machining process itself to characterize the behavior of the machined material.

The flow stress models that describe the work material behavior as a function of temperature, strain and strain rate are considered highly necessary to represent work material constitutive behavior under high-speed cutting conditions for work materials. Unfortunately, sound theoretical models based on atomic level material behavior are far from being materialized as reported by Jaspers and Dautzenberg (2002). Therefore, semi empirical constitutive models are widely utilized. Among such models, the constitutive model proposed by Johnson and Cook (1983) describes the flow stress of a material with the product of strain, strain rate, and temperature effects that are individually determined as given in Eq. (29).

$$\sigma = \left[A + B \cdot \varepsilon^n\right] \cdot \left[1 + C \cdot ln\left(\frac{\dot{\varepsilon}}{\dot{\varepsilon}_0}\right)\right] \cdot \left[1 - \left(\frac{T - T_0}{T_m - T_0}\right)^m\right] \tag{29}$$

In the Johnson-Cook constitutive model (Jaspers and Dautzenberg 2002), the parameter A is the initial yield strength of the material at room temperature and a strain rate of 1 s^{-1} and represents the plastic equivalent strain. The equivalent plastic strain rate $\dot{\varepsilon}$ is normalized with a reference strain rate $\dot{\varepsilon}_0$. The temperature term in the Johnson-Cook model reduces the flow stress to zero at the melting temperature of the work material T_m, leaving the constitutive model with no temperature effect. In general, the constants A, B, C, n, and m of the model are fitted to the data obtained by several material tests conducted at low strains and strain rates and at room temperature as well as the split Hopkinson pressure bar (SHPB) tests at strain rates up to 10^4 s^{-1} and at temperatures up to 600°C.

Different approaches have been used to identify the parameters for the rheology of the machined material expressed by the of Johnson-Cook model. Tounsi *et al*. (2002) applied the method of least squares estimation. Özel and Zeren (2006) used a nonlinear regression based on the Gauss-Newton algorithm. Aviral and Martin (2012) in their work an inverse identification method for Johnson–Cook model parameters is proposed. Chip shapes and cutting forces are used to define the error function. Parameters (A, B, n) are re-identified for two different starting points. Chip shapes, cutting forces and adiabatic stress–strain curves match very well.

4. Comparison of simulations to experiments

4.1 Determining the constants A, B, C, m, n to the constitutive equation to the Johnson Cook model

From the use of the test results on the orthogonal cutting whose contents included cutting force F_c and thrust force F_t values as well as the chip thickness t_1, we have programmed in MATLAB, the Johnson-Cook model by using nonlinear regression to solution based on the Levenberg-Marquardt algorithm change Bates and Watts (1988) for a better convergence, to determine the

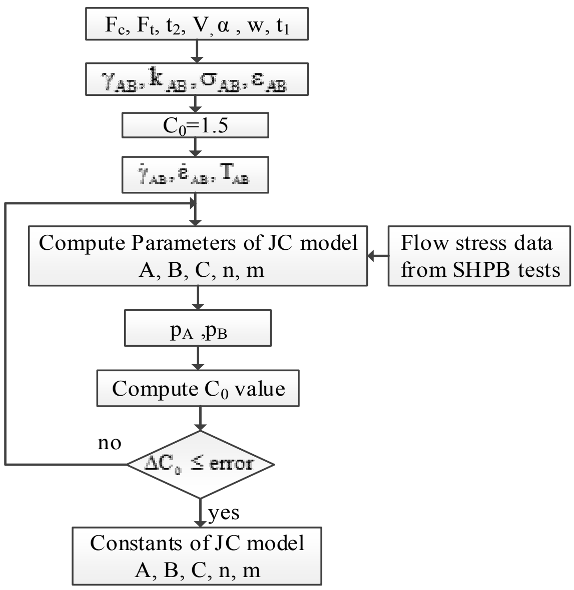

Fig. 2 Flow chart for the methodology to determine the constants of Johnson-Cook constitutive model

Table 1 Computed constants of Johnson-Cook flow stress model

	A	*B*	*C*	*n*	*m*
Experimental parameters (Jaspers and Dautzenberg 2002)	553.100	600.800	0.0134	0.2340	1.0000
Computed parameters	522.6828	750.9419	0.0111	0.2152	0.7762

constants *A*, *B*, *C*, *m*, *n* constitutive equation of this model. The proposed methodology has been tested for the machining of to 0.38% carbon steel. Necessary parameters for the simulation are taken from Tounsi *et al*. (2002). Stress fields data SHPB tests adopted by Jasper and Dautzenberg (2002) is determined under the conditions of orthogonal cutting. An iterative process solves C_0 parameter and the constants of Johnson-Cook constitutive model are calculated using the flowchart presented in Fig. 2.

Table 1, reports the constants of Johnson-Cook material model for work flow stress for 0.38% carbon steel obtained experimentally by testing to Hopkinson Pressure Bar of Jaspers and Dautzenberg (2002), and the computed parametersd.

There has been a good prediction of the constants of Johnson-Cook coefficients versus data experimentally.

4.2 Comparison of modified model with Oxley's original model for 0.38 % carbon steel

To improve the Oxley's model (1989), we followed in our modeling the following steps: Initially, we considered the Oxley's algorithm in its original version Oxley (1989) under the MATLAB and then it was simulated for orthogonal cutting conditions shown in Table 2. Note that the uniaxial flow stress (σ_1) and strain-hardening index (n) were introduced into the program as numerical tables because their evolutions are given by Oxley in the form of graphs.

The developed flowchart uses three main nested loops: the first relates to the thickness of the secondary shear zone, the second to the strain rate constant, and the third loop is for the determination of shear angle. In a second step and once the simulation, results were obtained and compared with those obtained by Oxley's model; we substituted in the same program by the constitutive equation of Johnson-Cook model Eq. (29), expressed by the equation empirical law Eq. (27). To reduce the computation time, the determination of average temperatures in primary and secondary shear zones and the constant of the strain rate constant uses the Newton-Raphson.

Table 2 Orthogonal cutting conditions and measured process variables for 0.38% carbon steel Oxley (1989)

Tool rake angle (α)	-5°
Cutting velocity (V)	100, 200, 300 and 400 m/min
Undeformed chip thickness (t_1)	0,125 ; 0,25 and 0,5 mm/tr
Width of cut (w)	4 mm
Machined material	0.38% carbon steel v = 0,09; $\dot{\varepsilon}_0$ = 1 s^{-1}; T_0 = 25 °C; ρ = 7862 kg/m^3 A = 553,1 MPa; B = 600,8 MPa; C = 0,0134 n = 0,234; m = 1; T_m = 1460°C

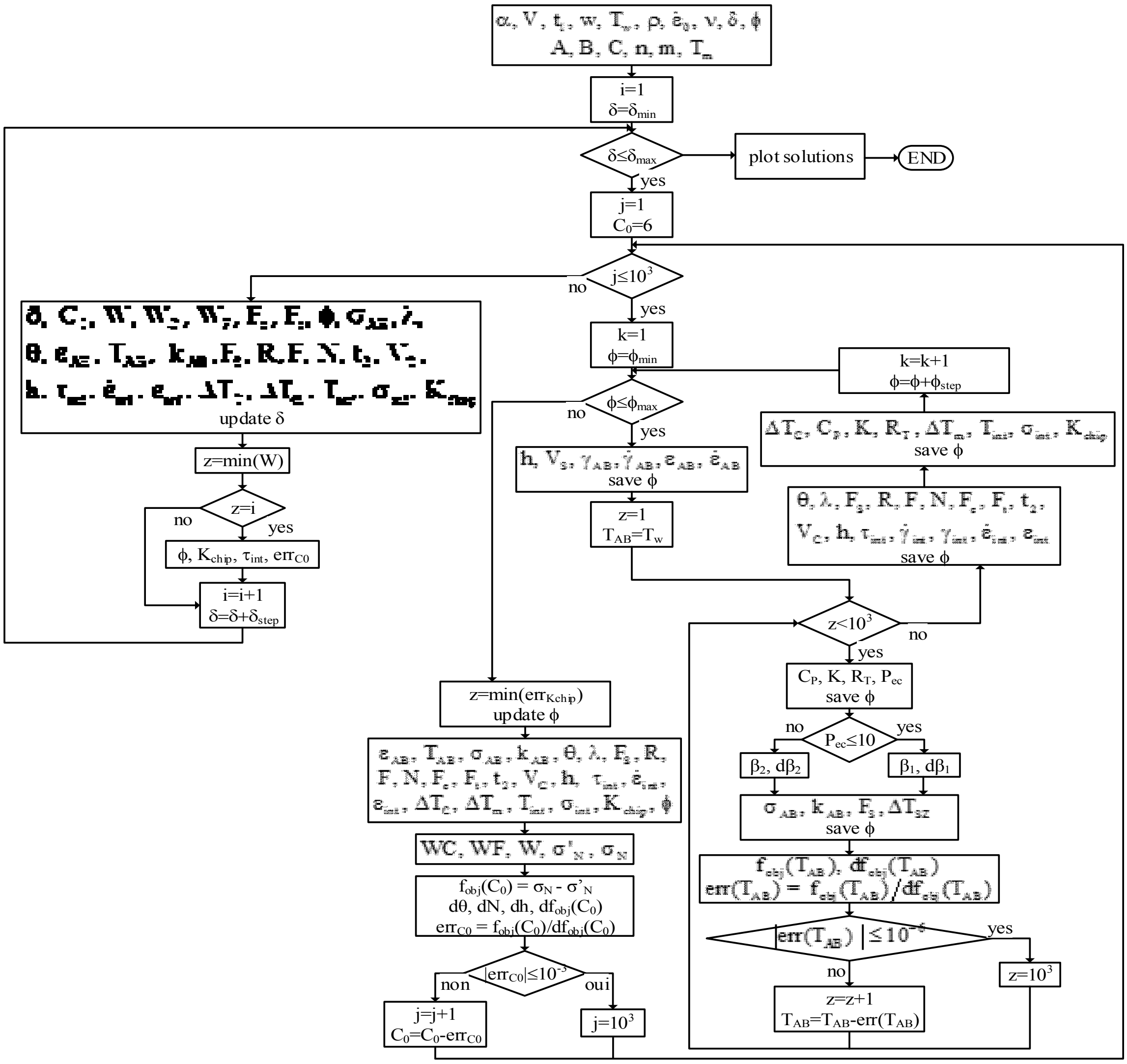

Fig. 3 Flowchart for the Oxley modified model

The flowchart summarizing these changes is presented in the Fig. 3.

Figs. 4(a)-(b)-(c), shows a comparison of the simulation results obtained through the Oxley's model and Oxley's modified model using the Johnson-Cook model to those from experimentation to cutting force F_c and thrust force F_t.

Despite measurement errors that can occur on the experimental results (wear of the cutting tool, for example), we note that the Oxley modified model provides a good prediction given that the average differences are low.

We note that the Oxley modified model provides very good results compared to the experiment. In addition, we find that an increasing of the undeformed chip thickness leads to an increase of cutting force F_c, thrust force F_t and the chip thickness t_2 for a fixed cutting velocity; by cons,

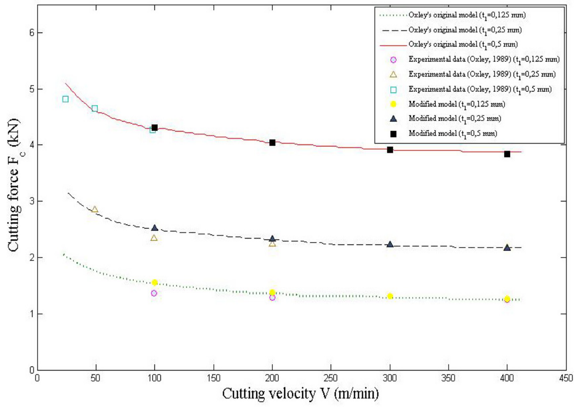

(a)

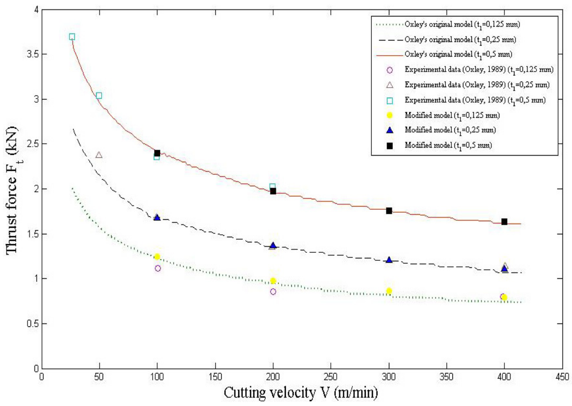

(b)

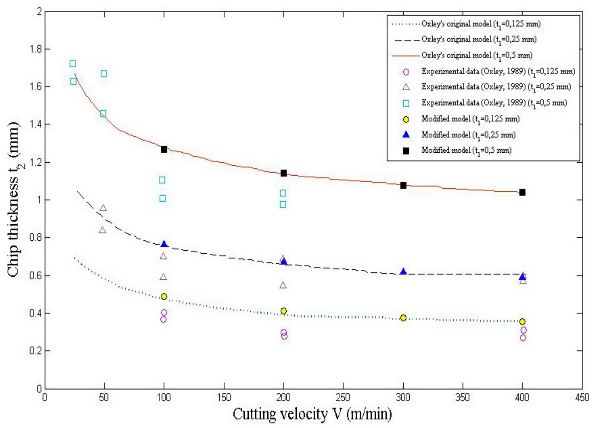

(c)

Fig. 4 Comparison of predicted : (a) cutting force; (b) thrust force; (c) chip thickness and the experimental data of Oxley (1989) with the predicted of Oxley modified for 0.38% carbon steel (α = -5)

Table 3 Computed results at primary and secondary deformation zones for 0.38% carbon steel (t_1 = 0,125 mm/tr; w = 4 mm; $\alpha = -5°$)

V (m/min)	σ_{AB} (MPa)	σ_{int} (MPa)	T_{AB} (°C)	T_{int} (°C)	ϕ (°)	h (mm)
100	1131,98	854,034	334,170	894,540	15,65	0,5087
200	1138,40	808,744	324,439	1022,48	18,20	0,4181
300	1145,55	778,324	315,261	1104,39	19,70	0,3766
400	1150,86	753,141	310,333	1169,60	20,75	0,3515

increased cutting velocity causes a decrease in these quantities for an undeformed chip thickness and width of cut by fixed step.

Tables 2-3-4 refer to variations in average stresses, average temperatures and geometric quantities in terms of the cutting velocity and undeformed chip thickness.

Table 4 Computed results at primary and secondary deformation zones for 0.38% carbon steel (t_1 = 0,125 mm/tr; w = 4 mm; $\alpha = -5°$)

V (m/min)	σ_{AB} (MPa)	σ_{int} (MPa)	T_{AB} (°C)	T_{int} (°C)	ϕ (°)	h (mm)
100	1109,13	772,672	310,131	976,69	18,85	0,7985
200	1121,40	715,529	297,495	1111,1400	21,45	0,6726
300	1127,60	677,005	292,869	1201,94	22,85	0,6179
400	1131,92	647,008	290,189	1277,78	23,85	0,5831

Table 5 Computed results at primary and secondary deformation zones for 0.38% carbon steel (t_1 = 0,5 mm/tr; w = 4 mm; $\alpha = -5°$)

V (m/min)	σ_{AB} (MPa)	σ_{int} (MPa)	T_{AB} (°C)	T_{int} (°C)	ϕ (°)	h (mm)
100	1093,05	680,419	286,415	1059,55	22,05	1,2965
200	1103,36	611,775	280,253	1212,93	24,45	1,1277
300	1109,23	569,058	278,547	1312,97	25,75	1,0509
400	1113,37	537,451	278,173	1389,17	26,60	1,0052

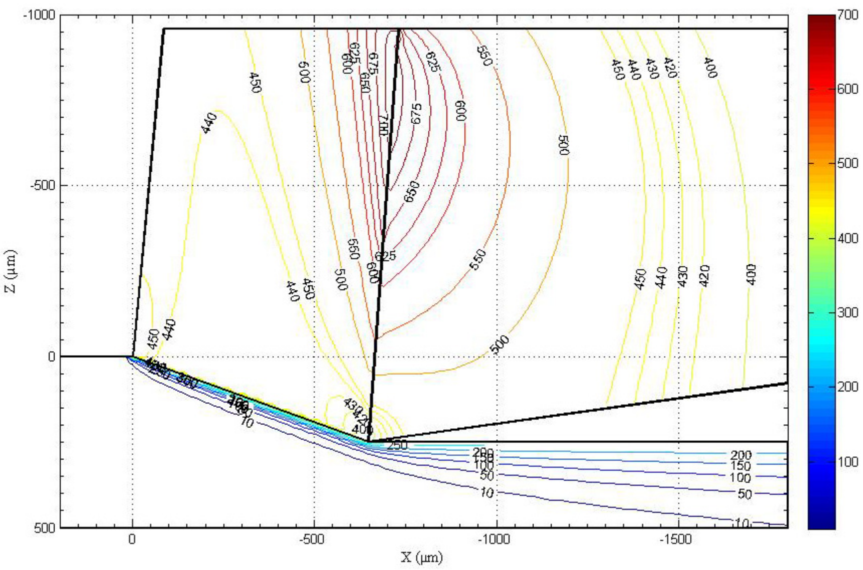

Fig. 5 Temperature distributions for NE 9445 steel

4.3 Simulation of the Komanduri and Hou developed model

We will now proceed to the simulation of Komanduri and Hou modified model Karas *et al.* (2013), under the MATLAB, to the temperature map at the tool-chip-workpiece interface.

The model input parameters such as shear angle (ϕ); the chip velocity (V_c); shear velocity (V_s); tool-chip interface length (h) and others geometric quantities in primary and secondary shear zones; cutting and thrust forces components (F_c, F_t), normal, friction forces at tool-chip interface

(*F*, *N*) are determined from the Oxley's modified model to allow, for the plot following temperatures maps in the cutting zones.

The temperature map Fig. 5, show the temperature distributions in the tool-chip-workpiece interface due to combined heat sources effects of in the primary and secondary shear zones.

The temperature map, confronted with those provided by the developments of Komanduri and Hou (2001), seem very promising.

5. Conclusions

In this paper, we have changed in a first step, and simulated the Oxley's original model by integrating the constitutive equation of Johnson-Cook model; it offers the possibility of its insertion in the adaptive control applications of the machining process. The calculations are more complex but then lead to better results. The comparative study showed reasonable deviations. The choice of the parameter C_0 and variable calibrating convergence tests are difficult, therefore, the resolution of these drawbacks was used the method of Newton-Raphson.

In this study, we also simulated the Komanduri and Hou's thermal model modified by Karas *et al*. (2013) in order to predict the temperature maps in the tool-chip-workpiece interaction in one axis system under fixed machining conditions. The results obtained are very promising in the field of prediction of the temperature distribution in the cutting zones.

In addition to the separate validation of two modified models, we want a combination between the two models for the same machining conditions: the first allows the prediction of cutting forces and geometrical quantities; these results will then be injected into the second model to predict the temperature distributions in the tool-chip-workpiece interaction.

References

Adibi-Sedeh, A.H., Madhavan, V. and Bahr, B. (2003), "Extension of Oxley's analysis of machining to use different material models", *J. Manuf. Sci. Eng.*, **125**(4), 656-666.

Aviral, S. and Martin, B. (2012), "Determination of Johnson-Cook parameters from machining simulations", *Computat. Mater. Sci.*, **52**(1), 298-304.

Bates, D. and Watts, D. (1988), *Nonlinear Regression Analysis and its Applications*, Wiley, New York, NY, USA, pp. 271-272.

Bogdan, P.N. and Milan, D.E. (2014), "Cutting temperature measurement and material machinability", *Therm. Sci.*, **18**(1), S259-S268.

Boothroyd, G. (1963), "Temperatures in orthogonal metal cutting", *Pro Institution of the Mechanical Engineers, G. I. London*, **177**(29), 789-810.

Chao, B.T. and Trigger, K.J. (1995), "Temperature distribution at tool-chip interface in metal cutting", *Transact. Am. Soc. Mech. Eng. ASME*, **75**(1), 1107-1121.

Gierlings, S. and Brockmann, M. (2013), "Analytical modeling of temperature distribution using potential theory by reference to broaching Nickel-Based alloys", *Adv. Mater. Res.*, **769**, 139-146.

Gierlings, S. and Brockmann, M. (2014), "Analytical model for tool temperature prediction in broaching Nickel-Based alloys", *Adv. Mater. Res.*, **1018**, 99-106.

Gilormini, P. (1982), "Contribution à la modélisation de la formation du copeau en usinage des métaux", Ph.D. Dissertation ; Ecole Nationale Supérieure des Mines de Paris, French.

Hahn, R.S. (1951), "On the temperature developed at the shear plane in the metal cutting process", *Proceedings of First US National Congress of Applied Mechanics*, Chicago, Illinois, June, pp. 661-666.

Hastings, W.F., Mathew, P. and Oxley, P.L.B. (1980), "A machining theory for predicting chip geometry, cutting forces etc. from material properties and cutting conditions", *Proceeding of the Royal Society of London* (GB), **A371**, pp. 569-587.

Jaspers, S.P.F.C. and Dautzenberg, J.H. (2002), "Material behavior in conditions similar to metal cutting: flow stress in the primary shear zone", *J. Mater. Process. Techno.*, **122**(2-3), 322-330.

Johnson, G.R. and Cook, W.H. (1983), "A constitutive model and data for metals subjected to large strains, high strain rates and high temperatures" *Proceedings of the 7th International Symposium on Ballistics*, The Hague, Netherlands, April, pp.541-547.

Karas, A., Bouzit, M. and Belarbi, M. (2013), "Development of a thermal model in the metal cutting process for prediction of temperature distributions at the tool-chip-workpiece interface", *J. Theor. Appl. Mech.*, **51**(3), 552-567.

Karpat, Y. and Özel, T. (2006), "Predictive analytical and thermal modeling of orthogonal cutting process – Part I: Predictions of tool forces, stresses, and temperature distributions", *J. Manuf. Sci. Eng.*, *ASEM*, **128**(2), 435-444.

Klocke, F., Gierlingsa, S., Brockmann, M. and Veselovac, D. (2014), "Force-based temperature modelling for surface integrity prediction in broaching nickel-based alloys", *Proceedings of the 2nd CIRP Conference on Surface Integrity* (*CSI*), Nottingham, England, May.

Komanduri, R. and Hou, Z.B. (2000), "Thermal modeling of the metal cutting process, Part I: temperature rise distribution due to Shear plane heat source", *Int. J. Mech. Sci.*, **42**(9), 1715-1752.

Komanduri, R. and Hou, Z.B. (2001a), "Thermal modeling of the metal cutting process, Part II: temperature rise distribution due to frictional heat source at the tool-chip interface", *Int. J. Mech. Sci.*, **43**(1), 57-88.

Komanduri, R. and Hou, Z.B. (2001b), "Thermal modeling of the metal cutting process, Part III: temperature rise distribution due to the combined effects of shear plane heat source and the tool-chip interface frictional heat Source", *Int. J. Mech. Sci.*, **43**(1), 89-107.

Lalwani, D.I., Mehta, N.K. and Jain, P.K. (2009), "Extension of Oxley's predictive machining theory for Johnson and Cook flow stress model", *J. Mater. Process. Technol.*, **209**(12-13), 5305-5312.

Liangshan, X., Jie W., Yiinye, G., Bin, L. and Ning, F. (2014), "Improvement of algorithm and prediction precision of an extended Oxley's theoretical model", *Int. J. Adv. Manuf. Technol.*, **77**(1), 1-13. DOI: 10.1007/s00170-014-6361.

Loewen, E.G. and Shaw, M.C. (1954), "On the analysis of cutting tool temperatures", *Transact. Am. Soc. Mech. Eng. ASEM*, **76**(2), 217-231.

Merchant, M.E. (1945), "Mechanics of the metal cutting process. I. Orthogonal cutting and a type 2 chip", *J. Appl. Phys.*, **16**(5), 267-279.

Oxley, P.L.B. (1989), *The Mechanics of Machining*: *An Analytical Approach to Assessing Machinability*, Ellis Horwood Ltd., England.

Oxley, P.L.B. and Hastings, W.F. (1975), "Minimum work as a possible criterion for determining the frictional conditions at the tool/chip interface in machining", *Proc. Instn. Mech. Engrs*, **282**(A1310), 565-584.

Özel, T. and Zeren, E. (2006), "A methodology to determine work material flow stress and tool-chip interfacial friction properties by using analysis of machining", *J. Manuf. Sci. Eng.*, **128**(1), 119-129.

Tounsi, N., Vincenti, J., Otho, A. and Elbestawi, M.A. (2002), "From the basic mechanics of orthogonal metal cutting toward the identification of the constitutive equation", *Int. J. Mach. Tools Manuf.*, **42**(12), 1373-1383.

Trigger, K.J. and Chao, B.T. (1951), "An analytical evaluation of metal cutting temperature", *Transact. Am. Soc. Mech. Eng. ASME*, **73**, 57-68.

CC

Nomenclature

A	plastic equivalent strain in Johnson-Cook constitutive model
B	strain related constant in Johnson-Cook constitutive model
C	strain-rate sensitivity constant in Johnson-Cook constitutive model
C_0	strain rate constant proposed by Oxley
C_p	specific heat of workpiece material
F	friction force at the tool-chip interface
F_C, F_T	cutting and thrust force components
F_F, F_N	frictional and normal force components at tool rake face
F_S	shear force to the shear force components at *AB*
f_{obj}	objective function
h	tool-chip interface length
K	thermal conductivity
k_{AB}	shear flow stress on *AB*
k_{chip}	shear flow stress in chip at tool-chip interface
l	length of shear plane *AB*
m	thermal softening parameter in Johnson-Cook constitutive model
n	strain-hardening parameter in Johnson-Cook constitutive model
p_A	hydrostatic pressure at the free surface of the nominal shear plane
p_B	hydrostatic pressure at the tool tip
P_e	Peclet number
N	normal force at tool-chip interface
R	resultant cutting force
R_T	nondimensional thermal number of work material
t_1	undeformed chip thickness
t_2	chip thickness
T	temperature
T_{AB}	temperature along *AB*
T_{int}	average temperature along tool-chip interface
T_m	melting temperature of the work material
T_{mod}	velocity modified temperature
T_0	reference temperature
T_w	temperature of the uncut work material
V	cutting velocity,
V_c	chip velocity

V_s	shear velocity
W	equivalent mechanical energy
W_c	shear energy per volume unit
W_f	energy of friction per volume unit
ΔT_c	average temperature rise in chip
ΔT_M	maximum temperature rise in chip
ΔT_{SZ}	temperature rise in shear zone
w	width of cut
α	tool rake angle
β	proportion of the heat conducted into work material
δ	ratio of tool-chip interface plastic zone thickness to chip thickness
ε	equivalent strain
ε_{AB}	equivalent strain at *AB*
$\dot{\varepsilon}_{AB}$	equivalent strain-rate at *AB*
$\dot{\varepsilon}_{\text{int}}$	equivalent strain-rate at tool–chip interface
$\dot{\varepsilon}_0$	reference strain-rate in Johnson and Cook flow stress model
ϕ	shear angle
γ_{AB}	shear strain along *AB*
$\dot{\gamma}_{AB}$	shear strain-rate along *AB*
$\dot{\gamma}_{\text{int}}$	shear strain-rate at tool–chip interface
θ	angle between the resultant cutting force, *R* and *AB*
λ	average friction angle at tool – chip interface
ρ	density of workpiece material
σ	flow stress
σ_N	normal stress at tool–chip interface calculated from resultant force *R*
σ'_N	normal stress calculated using stress boundary condition at *B*
σ_{AB}	effective flow stress at *AB*
σ_{int}	frictional shear stress at the tool-chip interface
τ_{int}	shear stress at tool-chip interface